Human Molecular Genetics, 2015, 1–10

doi: 10.1093/hmg/ddv473
Advance Access Publication Date: 00 2015
Original Article

ORIGINAL ARTICLE

MRI phenotypes with high neurodegeneration are associated with peripheral blood B-cell changes

Manuel Comabella[1,†,*], Ester Cantó[1,†], Ramil Nurtdinov[1], Jordi Río[1], Luisa M. Villar[3,4], Carmen Picón[3,4], Joaquín Castilló[1], Nicolás Fissolo[1], Xavier Aymerich[2], Cristina Auger[2], Alex Rovira[2] and Xavier Montalban[1]

[1]Servei de Neurologia-Neuroimmunologia, Centre d'Esclerosi Múltiple de Catalunya (Cemcat), Institut de Recerca Vall d'Hebron (VHIR), [2]Unitat de RM, Servei de Radiologia, Hospital Universitari Vall d'Hebron, Universitat Autònoma de Barcelona, Barcelona, Spain, [3]Department of Neurology and [4]Department of Immunology, Hospital Universitario Ramón y Cajal, Instituto Ramón y Cajal de Investigacion sanitaria, Madrid, Spain

*To whom correspondence should be addressed at: Unitat de Neuroimmunologia Clínica, CEM-Cat. Edif. EUI 2ª planta, Hospital Universitari Vall d'Hebron. Pg. Vall d'Hebron 119-129 08035 Barcelona, Spain. Tel: +34 932746834; Fax: +34 932746084; Email: manuel.comabella@vhir.org

Abstract

Little is known about the mechanisms leading to neurodegeneration in multiple sclerosis (MS) and the role of peripheral blood cells in this neurodegenerative component. We aimed to correlate brain radiological phenotypes defined by high and low neurodegeneration with gene expression profiling of peripheral blood mononuclear cells (PBMC) from MS patients. Magnetic resonance imaging (MRI) scans from 64 patients with relapsing-remitting MS (RRMS) were classified into radiological phenotypes characterized by low ($N = 27$) and high ($N = 37$) neurodegeneration according to the number of contrast-enhancing lesions, the relative volume of non-enhancing black holes on T1-weighted images, and the brain parenchymal fraction. Gene expression profiling was determined in PBMC using microarrays, and validation of selected genes was performed by polymerase chain reaction (PCR). B-cell immunophenotyping was conducted by flow cytometry. Microarray analysis revealed the B-cell specific genes *FCRL1*, *FCRL2*, *FCRL5* (Fc receptor-like 1, 2 and 5 respectively), and *CD22* as the top differentially expressed genes between patients with high and low neurodegeneration. Levels for these genes were significantly down-regulated in PBMC from patients with MRI phenotypes characterized by high neurodegeneration and microarray findings were validated by PCR. In patients with high neurodegeneration, immunophenotyping showed a significant increase in the expression of the B-cell activation markers CD80 in naïve B cells (CD45+/CD19+/CD27−/IgD+), unswitched memory B cells (CD45+/CD19+/CD27+/IgD+), and switched memory B cells (CD45+/CD19+/CD27+/IgD−), and CD86 in naïve and switched memory B cells. These results suggest that RRMS patients with radiological phenotypes showing high neurodegeneration have changes in B cells characterized by down-regulation of B-cell-specific genes and increased activation status.

Introduction

Multiple sclerosis (MS) pathogenesis is characterized by at least two major processes, inflammation and neurodegeneration (1). Whereas inflammation predominates in the initial phases of the disease, the neurodegenerative component is usually more prominent in the late stages of MS, although it can be present early in the disease course (2). Current available therapies in MS have proven to be highly effective to suppress the inflammatory component of the disease. In contrast, the mechanisms leading to neurodegeneration are less well understood and,

[†]M.C. and E.C. contributed equally to this work.

Received: September 1, 2015. **Revised and Accepted:** November 15, 2015

unfortunately, existing therapies remain largely ineffective in patients where the neurodegenerative component dominates (3,4). In this context, a better understanding of the mechanisms of neurodegeneration occurring in MS may help to identify molecular targets that set the rationale for the design of specific and effective therapeutic approaches to prevent neurodegeneration.

A large number of gene expression profiling studies using DNA microarrays have been conducted in peripheral blood cells from MS patients pursuing the identification of specific blood transcriptomic patterns that may help to differentiate MS patients from healthy individuals or patients with other autoimmune conditions, or between MS patients with different clinical forms and activity phases of the disease (5). In the present study, we aimed to gain more insight into the mechanisms of neurodegeneration operating in MS by correlating gene expression microarray findings in peripheral blood mononuclear cells (PBMC) from MS patients with magnetic resonance imaging (MRI) phenotypes characterized by high and low neurodegenerative components.

Results

B-cell specific genes are differentially expressed between patients with high and low neurodegeneration

Gene expression profiling was first determined in PBMC isolated from relapsing-remitting MS (RRMS) patients with MRI phenotypes characterized by high and low neurodegenerative components, as described in Materials and Methods. Analysis of microarray data revealed B-cell specific genes among the top differentially expressed genes between patients with high and low neurodegeneration: *FCRL1*, *FCRL2*, *FCRL5* (Fc receptor-like 1, 2 and 5 respectively), and *CD22* (Table 1). The full list of additional differentially expressed genes with P-values <0.01 is provided as Supplementary Material, Table S1.

As shown in Fig. 1A, mRNA expression levels for these genes were significantly lower in PBMC from patients with MRI phenotypes characterized by a high neurodegenerative component compared with PBMC from patients with low neurodegeneration.

PCR validation of *FCRL1*, *FCRL2*, *FCRL5*, *CD22* as down-regulated genes in patients with high neurodegeneration

We next approached the validation of differentially expressed B-cell specific genes obtained with microarrays by means of real-time PCR relative quantification in a subgroup of RRMS patients. As depicted in Figure 1B, microarray findings for *FCRL1*, *FCRL2*, *FCRL5*, *CD22* were validated by PCR and mRNA expression levels for these genes were significantly down-regulated in PBMC from patients with high neurodegeneration compared with patients with low neurodegeneration.

B cells are more activated and express more IL-6 in RRMS patients with high neurodegeneration

Considering the immunomodulatory B-cell-related role of *FCRL1*, *FCRL2*, *FCRL5* and *CD22*, and their preferential expression in B cells (Supplementary Material, Fig. S1), we next aimed to investigate the activation status of B cells from RRMS patients with MRI phenotypes characterized by high neurodegeneration. To rule

Table 1. Top differentially expressed genes obtained with microarrays in PBMC from RRMS patients with high and low neurodegenerative components in brain MRI

Affymetrix probe set	Symbol	Description	LogFC	P value
221239_s_at	**FCRL2**	Fc receptor-like 2	−1.083	5.3×10^{-5}
1563674_at	**FCRL2**	Fc receptor-like 2	−1.069	5.0×10^{-4}
243968_x_at	**FCRL1**	Fc receptor-like 1	−1.063	5.6×10^{-4}
204287_at	SYNGR1	Synaptogyrin 1	1.027	6.6×10^{-4}
224558_s_at	MALAT1	Metastasis associated lung adenocarcinoma transcript 1 (non-protein coding)	−1.049	8.1×10^{-4}
223176_at	KCTD20	Potassium channel tetramerisation domain containing 20	1.029	8.8×10^{-4}
235982_at	**FCRL1**	Fc receptor-like 1	−1.083	9.3×10^{-4}
241401_at	C4orf12	Chromosome 4 open reading frame 12	1.045	1.2×10^{-3}
240261_at	TOM1L1	Target of myb1 (chicken)-like 1	−1.037	1.3×10^{-3}
38521_at	**CD22**	CD22 molecule	−1.037	1.4×10^{-3}
204581_at	**CD22**	CD22 molecule	−1.048	1.5×10^{-3}
207819_s_at	ABCB4	ATP-binding cassette, sub-family B (MDR/TAP), member 4	−1.062	2.1×10^{-3}
210538_s_a	BIRC3	Baculoviral IAP repeat-containing 3	−1.038	2.1×10^{-3}
217512_at	KNG1	Kininogen 1	1.041	2.4×10^{-3}
Affymetrix probe set	Symbol	Description	LogFC	P value
202732_at	PKIG	Protein kinase (cAMP-dependent, catalytic) inhibitor gamma	−1.043	2.5×10^{-3}
1559059_s_at	ZNF611	Zinc finger protein 611	1.034	2.6×10^{-3}
1560683_at	BCL8	B-cell CLL/lymphoma 8	−1.039	2.8×10^{-3}
228485_s_at	SLC44A1	Solute carrier family 44, member 1	1.048	3.0×10^{-3}
212423_at	ZCCHC24	Zinc finger, CCHC domain containing 24	1.030	3.0×10^{-3}
1568706_s_at	AVIL	Advillin	−1.041	3.1×10^{-3}
230718_at	HSF5	Heat shock transcription factor family member 5	−1.055	3.1×10^{-3}
224404_s_at	**FCRL5**	Fc receptor-like 5	−1.087	3.2×10^{-3}
238417_at	PGM2L1	phosphoglucomutase 2-like 1	−1.025	3.2×10^{-3}
204004_at	PAWR	PRKC, apoptosis, WT1, regulator	−1.056	3.3×10^{-3}
224406_s_at	**FCRL5**	Fc receptor-like 5	−1.058	3.5×10^{-3}

Analysis was adjusted by age. B-cell specific genes are shown in bold. LogFC: mean log fold change, and positive/negative values indicate higher/lower gene expression levels in PBMC from patients with high neurodegenerative component versus patients with low neurodegenerative component respectively. None of the P values was <0.05 after correction for multiple testing.

out that the transcriptional differences observed for B-cell specific genes were not due to differences in the number of B cells, we analyzed the relative percentage of B cells in patients with high and low neurodegeneration. As shown in Figure 2A, the percentage of CD19+ B cells in PBMC was comparable between both groups of patients ($P = 0.472$). Immunophenotyping of the B-cell population revealed a trend towards increased expression of the B-cell activation marker CD80 in CD19+ B cells from patients with high neurodegeneration ($P = 0.05$; Fig. 2B). Further B-cell-specific immunophenotyping showed a significant increase in the expression of CD80 in naïve B cells ($P = 0.04$), unswitched memory B cells ($P = 0.03$), and switched memory B cells ($P = 0.008$) in PBMC from patients with MRI phenotypes characterized by high neurodegeneration compared with patients with low neurodegeneration phenotypes (Fig. 2B). Expression of the B-cell activation marker CD86 was also found significantly increased in naïve B cells and switched memory B cells ($P = 0.04$ and $P = 0.02$ respectively; Fig. 2C) from patients with high neurodegeneration.

Immunophenotyping of the B-cell specific markers FCRL1, FCRL2 and CD22 did not reveal statistically significant differences between patients with high and low neurodegeneration for any of the B-cell populations analyzed (Supplementary Material, Table S2 shows the full list of variables included in the immunophenotyping).

Finally, intracellular cytokine determination by CD19+ B cells revealed a significantly higher expression of IL-6 by B cells from patients with high neurodegeneration compared with patients with low neurodegeneration ($P = 0.03$; Fig. 2D). No significant differences ($P < 0.05$) were observed between both groups of patients for TNF [mean percentage of CD19+ B cells expressing TNF (standard deviation): 21.9 (7.8) for patients with low neurodegeneration; 31.0 (19.3) for patients with high neurodegeneration] and IL-10 [mean percentage of CD19+ B cells expressing IL-10 (standard deviation): 1.0 (0.7) for patients with low neurodegeneration; 2.5 (2.1) for patients with high neurodegeneration].

Discussion

Little is known about the neurodegenerative mechanisms operating in MS patients. In an attempt to investigate a potential involvement of peripheral blood immune cells in the neurodegenerative component of the disease, brain MRI scans from RRMS patients were classified into radiological phenotypes characterized by high and low neurodegeneration and correlated with differentially

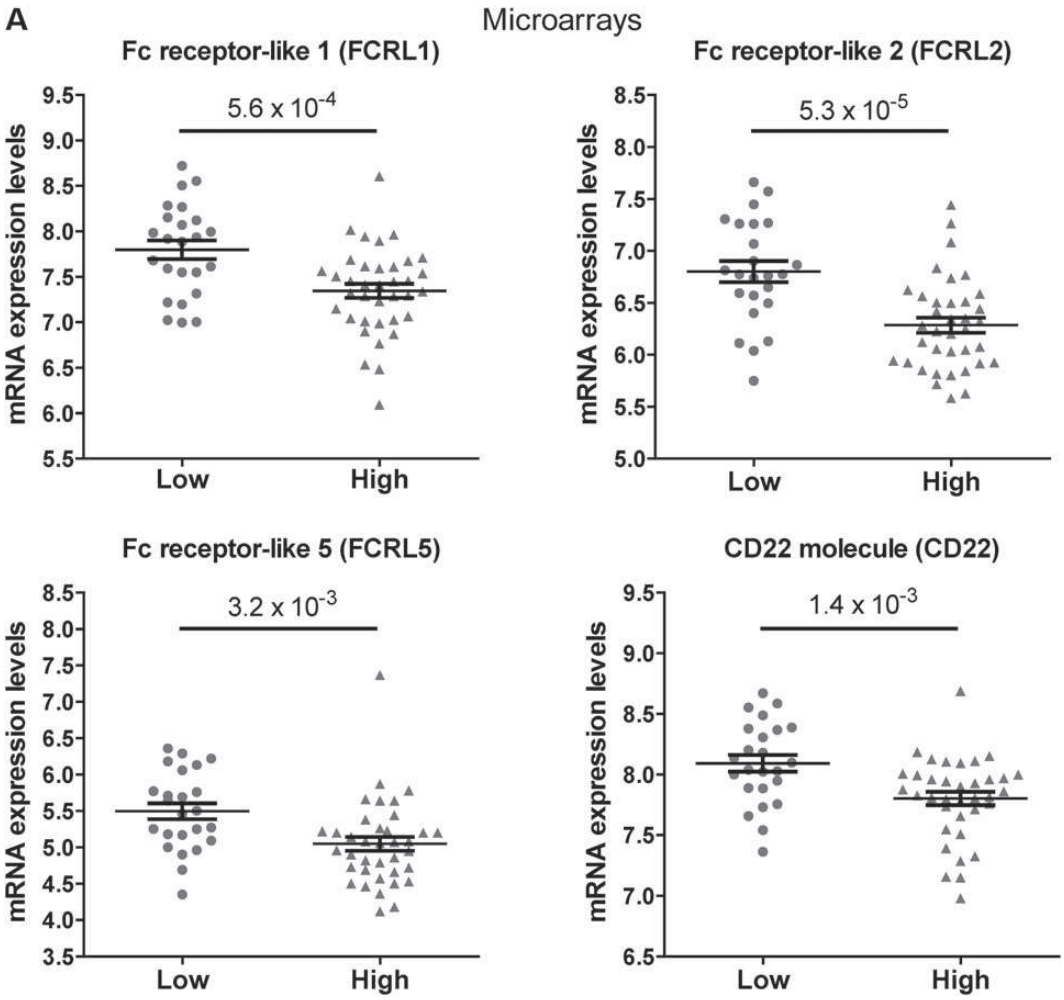

Figure 1. mRNA expression levels of differentially expressed B-cell specific genes in patients with high and low neurodegeneration. (**A**) Expression levels of *FCRL1*, *FCRL2*, *FCRL5*, *CD22* obtained with microarrays. Three samples from the low neurodegeneration group were not included for microarray analysis due to poor total RNA quality. (**B**) Validation of *FCRL1*, *FCRL2*, *FCRL5*, *CD22* by means of real-time PCR. Results are expressed as fold change in gene expression in PBMC from RRMS patients with high neurodegeneration relative to patients with low neurodegeneration.

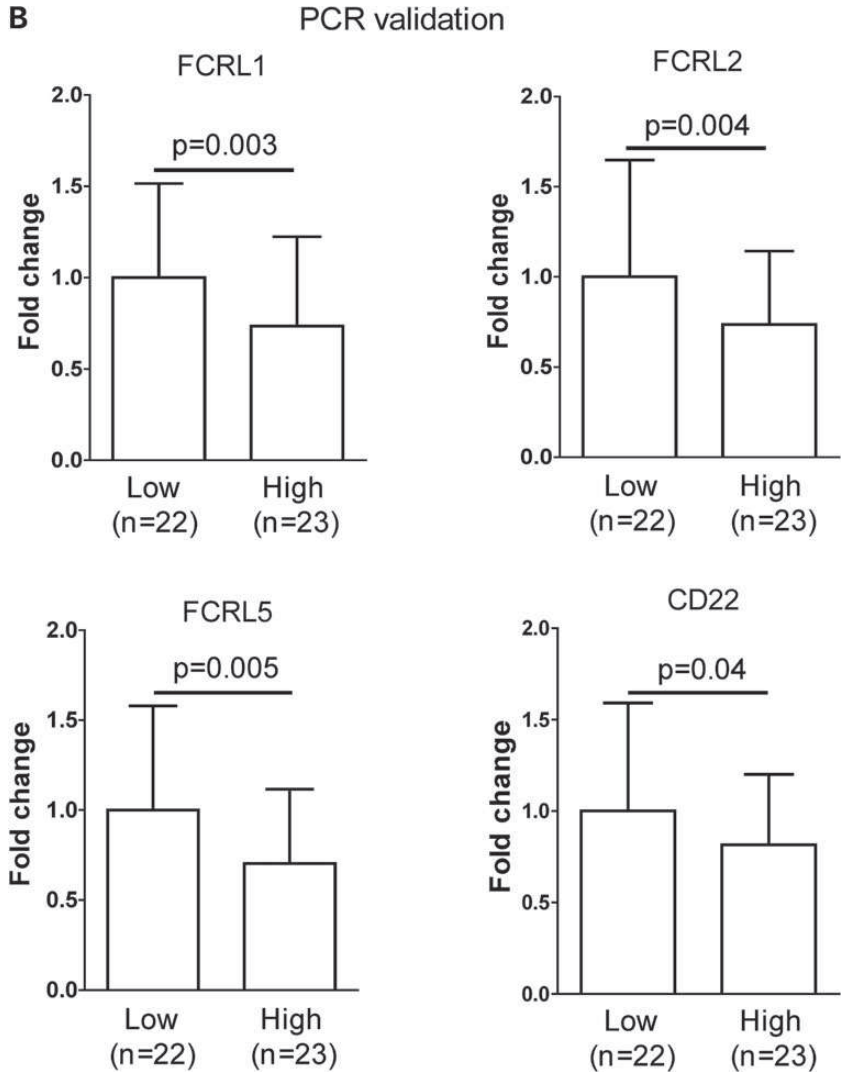

Figure 1. Continued

expressed genes observed in PBMC form patients using microarrays. Gene expression analysis pointed to the B-cell specific genes *FCRL1*, *FCRL2*, *FCRL5* and *CD22* as the top differentially expressed genes between MS patients with divergent radiological phenotypes, with lower expression in those patients whose brain MRI scans showed high neurodegeneration.

FCRL genes encode cell-surface membrane proteins preferentially expressed on B-lineage cells and containing both immunoreceptor tyrosine-based activation and inhibitory motifs (ITAM and ITIM, respectively) (6). The potential of FCRL molecules to deliver activating and/or inhibitory signals suggests that these receptors could influence B-cell signaling and hence play immunomodulatory roles in these cells (6). CD22 codes for a membrane glycoprotein expressed on B cells, which also contains ITIMs and functions as a co-receptor of the B-cell receptor (7). Interestingly, inhibitory roles in B-cell activation have been described for FCRL2 (8), FCRL5 (9) and CD22 (10). In our study, peripheral blood B cells were more activated in patients with high neurodegeneration, as revealed by the higher expression of CD80 in all B-cell subsets immunophenotyped, and CD86 in some B-cell populations. In addition, expression of the pro-inflammatory cytokine IL-6 was increased in B cells from patients with neurodegeneration.

It is generally accepted that B cells may contribute to the pathogenesis of MS in different ways: B cells differentiate to plasma cells which possibly secrete pathogenic antibodies that target oligodendrocytes and participate in the demyelination process (11); they may function as efficient antigen-presenting cells for the activation of T cells (12); and B cells may regulate inflammatory processes via secretion of pro-inflammatory (IL-6, TNF) and anti-inflammatory (IL-10) cytokines (12). The potential role of B cells in the neurodegenerative component of MS and disease progression is less understood. It is relevant to mention that together with T cells, B cells are abundant in subpial cortical lesions associated with plaque-like primary demyelination and neurodegeneration, a finding that is specific for MS and not observed in other inflammatory and non-inflammatory neurological conditions disorders (13). Furthermore, B-cell-enriched follicle-like aggregates have been reported in the meninges of patients with chronic progressive disease course and associated with large subpial cortical lesions, microglia activation and neuronal loss (14).

Our study associates changes at the transcriptional level in PBMC from MS patients with radiological phenotypes showing high neurodegeneration. The nature of top differentially

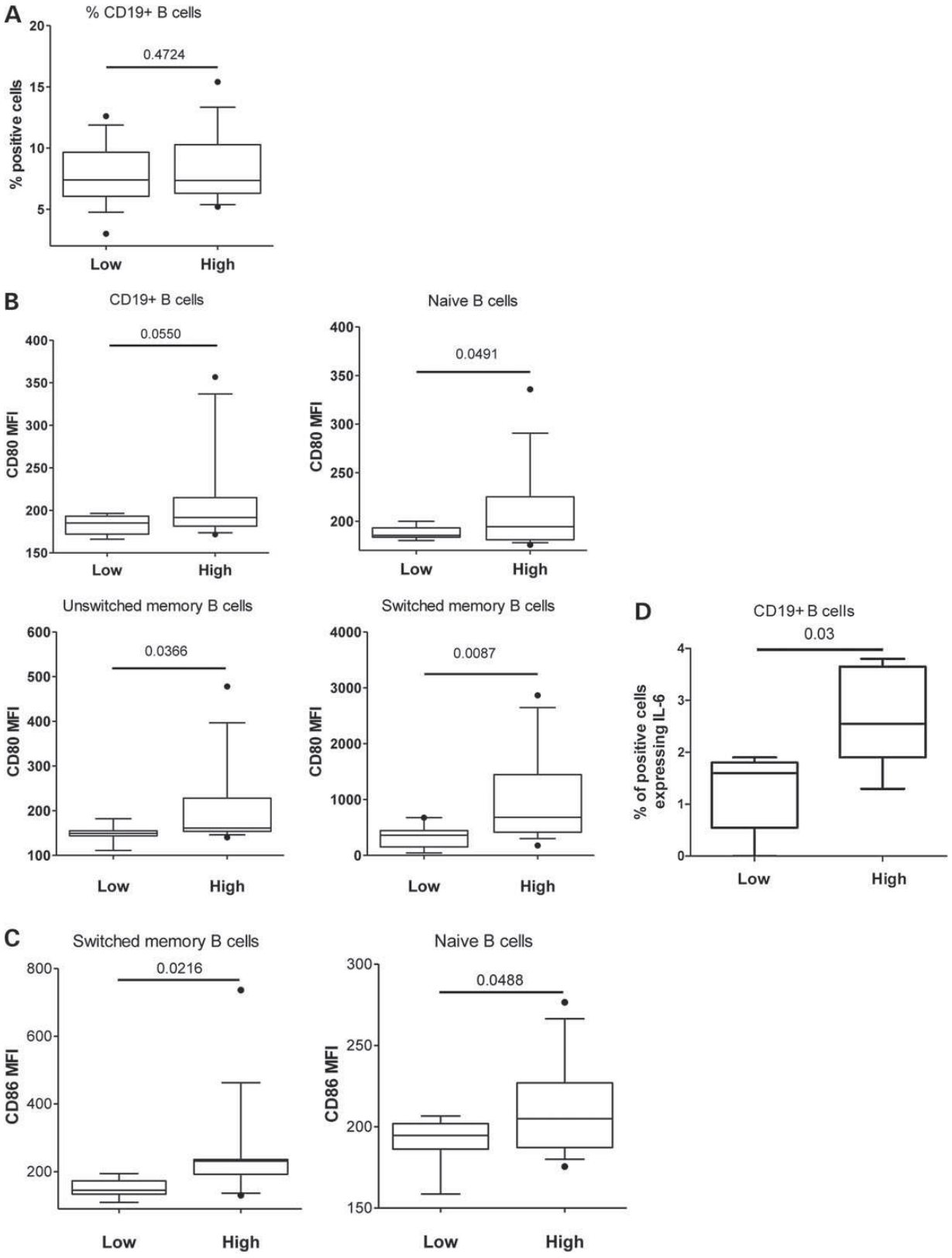

Figure 2. B-cell immunophenotyping in patients with high and low neurodegeneration. (**A**) Relative percentage of CD19+ B cells in PBMC. (**B**) Expression of the B-cell activation marker CD80 in the whole CD19+ B-cell population and in the different B-cell subpopulations. (**C**) Expression of the B-cell activation marker CD86 in naïve and switched memory B cells. (**D**) Percentage of CD19+ B cells expressing IL-6. Naïve B cells were considered as CD45+/CD19+/CD27−/IgD+. Unswitched memory B cells were considered as CD45+/CD19+/CD27+/IgD+. Switched memory B cells were considered as CD45+/CD19+/CD27+/IgD−. Analysis of flow cytometry immunophenotyping was adjusted by age. MFI, mean fluorescence intensity (median values). Low, patients with low neurodegeneration ($N = 17$ for A–C; $N = 5$ for D). High, patients with high neurodegeneration ($N = 18$ for A–C; $N = 6$ for D).

expressed genes and immunophenotyping point to B cells as the peripheral blood cell population altered in patients with high neurodegeneration. These findings are descriptive and only suggest an involvement of B cells in the neurodegenerative component of MS. How these B cell changes may translate into higher degrees of brain atrophy and tissue destruction is unknown and not addressed in the study. However, the positive effects of the B-cell depleting agent ocrelizumab in a recent Phase III clinical trial in patients with progressive disease (ORATORIO; NCT01194570) on the primary endpoint, confirmed disability progression sustained for ≥12 weeks, supports a role of B cells in the neurodegenerative component of the disease (unpublished data).

In our study, it is important to comment that findings in gene expression and immunophenotyping were not due to age differences between patients with high and low neurodegeneration, insomuch as statistical analysis was considering this covariate. Similarly, down-regulation of B cell genes was not secondary to a lower representation of B cells in patients with high neurodegeneration, since the percentage of CD19+ B cells in PBMC did not differ between both groups of patients. We failed to demonstrate a lower protein expression of FCRL1, FCRL2 and CD22 in the different B-cell subsets by flow cytometry in patients with high neurodegeneration, although factors such as lower sample size and differences in the sensitivities of the techniques used to measure the molecules (PCR versus flow cytometry) may well explain the negative findings.

In summary, the aggregate findings of the study suggest that RRMS patients whose brain MRI scans show high neurodegeneration have associated changes in the population of peripheral blood B cells characterized by down-regulation of B-cell-specific genes and higher activation status.

Materials and Methods

MRI analyses and patients

MRI of the brain was acquired on a 1.5 T superconductive magnet using a standardized protocol (2D fast spin-echo T2-weighted, and pre- and post-contrast (0.1 mmol/kg, 5 min delay) 2D spin-echo T_1-weighted sequences). For all sequences 46 interleaved contiguous axial sections were acquired with a 3-mm section thickness covering the whole brain, with an in-plane spatial resolution of ~1 × 1 mm.

In all patients, two experienced neuroradiologists visually assessed the presence and number of gadolinium (Gd) enhancing lesions on post-contrast T_1-weighted scans. Brain parenchymal fraction (BPF), a normalized brain volume measure, commonly used as a surrogate of whole-brain atrophy, was calculated on the pre-contrast T_1-weighted scans using a fully automated segmentation technique as previously described (15).

For calculating the non-enhanced T1 black hole volume we used an in-house automatic segmentation algorithm that measure the T1-lesion load from the initial T2-lesion segmentation that was used as lesion mask. T2 lesion segmentation was performed using a semiautomatic local thresholding contour technique (Dispimage, DL Plummer, University College, London, UK) or in case the lesion could not be outlined satisfactorily with this approach, by manual outlining. Relative T_1 black hole volume or black hole fraction (BHf) is expressed as the ratio of T_1 lesion volume to the T_2 lesion volume.

Due to the design of the present study, in which we used previously acquired MRI data, we could not use high resolution 3D T1-weigted images, which are probably the optimal sequence for calculating regional brain volumes due to the high contrast they provide between grey and white matter. However, the 2D sequence we used in this study, which is the standard of practice in many institutions, at least when 1.5 T magnets are used, is adequate for calculating global brain volume, and has been commonly used for that purpose in many clinical studies and clinical trials (16,17).

Figure 3 illustrates the MRI-based stratification algorithm applied to the study [modified from Bielekova *et al.* (18)]. In order to identify peripheral blood gene expression patterns associated with radiological phenotypes characterized by high tissue destruction and minimize the effect of inflammation on the neurodegenerative component, MRI scans were first classified into low inflammation and high inflammation phenotypes according to the number of contrast-enhancing lesions. Subsequent MRI analyses were performed on low inflammation radiological phenotypes which were defined by the presence of ≤1 Gd-enhancing lesions. MRI phenotypes with high neurodegenerative component were defined as follows: (i) the presence of BPF values <0.83; or (ii) BPF values ≥0.83 and presence of BHf values ≥10%. MRI phenotypes with low neurodegenerative component were defined by the presence of BPF values ≥0.83 and BHf values <10%. These cut-off values were selected, to separate the groups, based on a previous study that used similar techniques and T1-weighted sequences for calculating them (18).

The initial cohort comprised 108 RRMS patients with MRI examinations performed as part of a prospective study of patients receiving treatment with interferon-beta (IFNβ). MRI scans corresponded to the baseline determination before IFNβ and none of the patients had ever received treatment with immunomodulators or immunosuppressants before study entry. Sixty-four out of 108 RRMS patients had MRI phenotypes characterized by low inflammation and were included in the study. Of these, 27 patients had low and 37 patients high neurodegeneration phenotypes. Table 2 shows a summary of demographic and clinical characteristics of RRMS patients. Mean age of patients with high neurodegeneration phenotypes was significantly higher compared with patients with low neurodegeneration phenotypes.

The study was approved by the Hospital ethics committee, and all patients gave their informed consent.

Sample collection and gene expression microarrays

Peripheral blood was extracted in proximity to the MRI scans [mean days (standard deviation): 49.3 days (47.3) for patients with low neurodegeneration; 52.2 days (41.8) for patients with high neurodegeneration]. None of the patients received corticosteroid treatment within 1 month before MRI scans and blood collection. PBMC from patients were isolated by Ficoll-Isopaque density gradient centrifugation (Gibco BRL, Life Technologies LTD, UK) and stored in liquid nitrogen until used. Total RNA was extracted from PBMC using an RNeasy kit (Quiagen, Santa Clarita, USA) and hybridized to microarray expression chips (Affymetrix Human Genome U133A Plus 2.0 arrays) according to the manufactureŕs protocol (Affymetrix Inc., Santa Clara, CA, USA).

Statistical analysis of microarray data

Analysis of the expression data was carried out by using the Bioconductor packages for the R programming environment. All chips were explored one by one and checked for quality. Subsequently, data obtained from .CEL files were preprocessed using the RMA method (19) implemented in Affymetrix Expression Console software. Linear models for microarray data R package

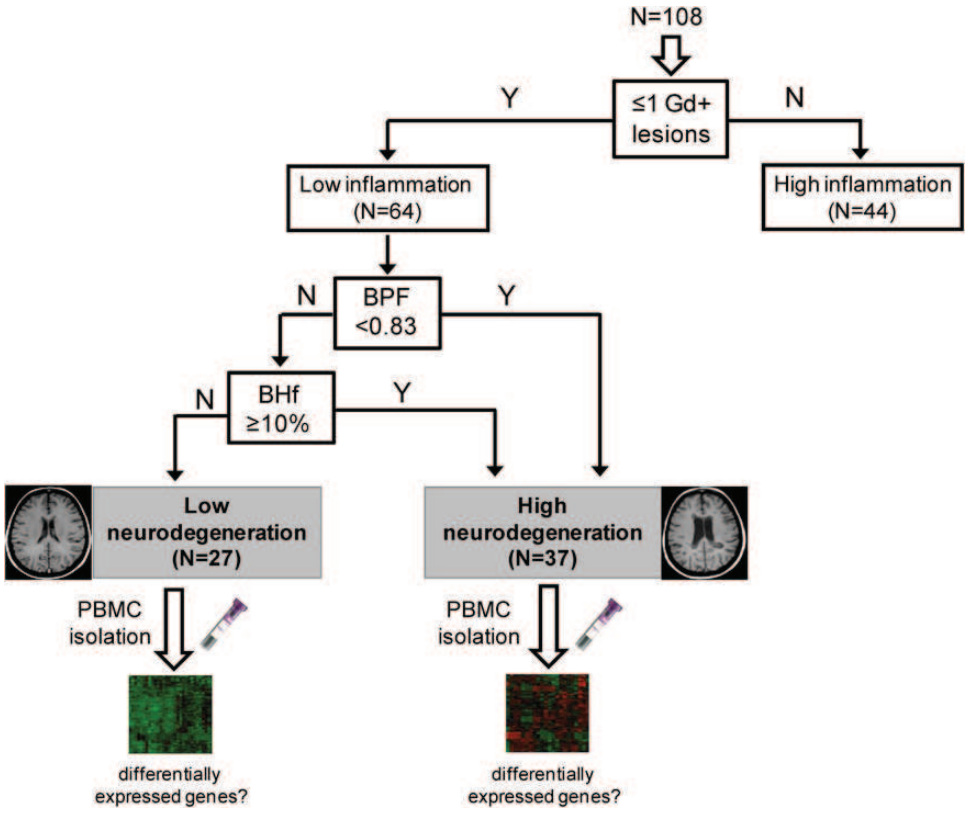

Figure 3. Stratification algorithm applied to brain MRI scans to identify radiological phenotypes with high and low neurodegeneration. To identify gene expression profiles specifically associated with the neurodegeneration component and exclude the effect of inflammation, only RRMS patients with low inflammation phenotypes (≤1 Gd+ lesions) were included in the study. Further stratification of low inflammation phenotypes into high and low neurodegeneration phenotypes was performed according to the combination of BPF and BHf, as detailed in the Materials and Methods. In patients with high and low neurodegeneration, PBMC were isolated and the gene expression profiling was determined from these cells by means of microrrays. BPF, brain parenchymal fraction; BHf: black hole fraction; Gd+ lesions, number of Gd-enhancing lesions; PBMC, peripheral blood mononuclear cells; Y (yes), indicates that the condition is satisfied; N (no), indicates that the condition is not fulfilled.

(20) were used to identify differentially expressed genes between RRMS patients with high and low neurodegeneration MRI phenotypes. Considering the statistically significant differences in age between both groups of patients, expression values for analysis were adjusted by age.

Validation of microarray data with real-time PCR

Expression levels of selected genes were determined by real-time quantitative reverse transcription PCR in a subgroup of 23 patients with high and 22 patients with low neurodegeneration phenotypes. As shown in Supplementary Material, Table S3, this subgroup of patients was representative of the original cohort used for gene expression profiling. Total RNA was obtained from the same samples that had been used for the microarrays. cDNA was synthesized from total RNA using the High Capacity cDNA Reverse Transcription (Applied Biosystems, Foster City, CA, USA). Amplifications were performed in duplicate using Taqman probes specific for *FCRL1*, *FCRL2*, *FCRL5* (Fc receptor-like 1, 2 and 5 respectively) and *CD22* (Applied Biosystems). The housekeeping gene *GAPDH* was used as an endogenous control. The threshold cycle (CT) value for each reaction, and the relative level of gene expression for each sample were calculated using the $2-\Delta\Delta CT$ method (21).

B-cell flow cytometry immunophenotyping and B-cell subpopulations

Immunophenotyping of B cells was performed in frozen PBMC from a subgroup of 18 patients with high and 17 patients with low neurodegeneration phenotypes. This cohort was representative of the original cohort used for microarray studies (Supplementary Material, Table S3). For B-cell surface marker staining PBMC were thawed at 37°C, blocked with human IgG for 20 min at room temperature, and labeled with optimal concentrations of anti-CD45-APC-Cy7, anti-CD19-PerCP-Cy5.5, anti-IgD-FITC, anti-CD27-APC, anti-FCRL1-PE, anti-FCRL2-PE, anti-CD22-PE, or the corresponding isotype controls for 30 min at room temperature. For B-cell activation assessment, PBMC were thawed at 37°C and labeled with optimal concentrations of anti-CD45-APC-Cy7, anti-CD19-PerCP-Cy5.5, anti-IgD-FITC, anti-CD27-APC, anti-CD80, anti-CD86 or the isotype controls for 30 min at room temperature. Samples were analyzed on a standard FACSCanto I instrument (Becton Dickinson, BD, New Jersey, USA). Analysis was performed using the BD FACSDiva software v.5.3. At least 20 000 lymphocyte-gated cells were analyzed for each sample.

B cells were classified into different subtypes according to the expression of their surface markers: (i) naïve B cells (CD45+/CD19+/CD27−/IgD+); (ii) memory B cells (CD45+/CD19+/CD27+); (iii) unswitched memory B cells (CD45+/CD19+/CD27+/IgD+); and (iv) switched memory B cells (CD45+/CD19+/CD27+/IgD−). FCRL1, FCRL2, CD22, CD80 and CD86 expression was evaluated in the abovementioned B-cell subpopulations. B-cell activation was investigated by examining CD80 and CD86 expression in the different B-cell subpopulations.

Regarding the statistical analysis of flow cytometry data, the observed values of cell counts and population frequencies were adjusted by age. For each observation, the Welch's two sample

Table 2. Demographic and clinical characteristics of RRMS patients with low and high neurodegeneration phenotypes in brain MRI

Baseline characteristics	Low	High	*P* value*
N	27	37	—
Age (years)	32.0 (6.7)	37.8 (8.9)	**0.005**
Female/male (% women)	21/6 (77.8)	25/12 (67.6)	0.370
Duration of disease (years)	3.7 (3.8)	5.5 (5.9)	0.169
EDSS[a]	1.9 (1.0–2.5)	2.3 (1.5–3.0)	0.075
Number of relapses[b]	1.8 (0.7)	1.9 (0.7)	0.580

Data are expressed as mean (standard deviation) unless otherwise stated.
[a]Data are expressed as mean (interquartile range).
[b]Refers to the number of relapses in the two previous years.
*Refers to *P* values obtained following comparisons between patients with low and high neurodegeneration phenotypes by means of Students *t*-test or Mann–Whitney's test depending on the applicability conditions (age, duration, EDSS and number of relapses) and χ^2 test (gender). Significant *P*-values are shown in bold.

t-test was applied and *P*-values <0.05 were considered statistically significant.

Intracellular cytokine production by B cells

Cytokine production by B cells was performed in frozen PBMC from a representative subgroup of 11 patients, 6 with high and 5 with low neurodegeneration phenotypes (Supplementary Material, Table S3). PBMC were thawed and suspended in 1 ml of RPMI 1640 medium supplemented with 10% fetal calf serum, 2 mM glutamine and 20 ng/ml of gentamycin (all from Gibco BRL, Karlsruhe, Germany) at a concentration of 10^6 cells/ml. To explore intracellular TNF-α and IL-6 production by B cells two 1 ml aliquots were cultured in the presence or absence of 50 ng/ml phorbol 12-myristate 13-acetate (PMA; Sigma-Aldrich) and 750 ng/ml ionomycin (Sigma-Aldrich). We added 2 μg/ml brefeldin A (GolgiPlug, BD Biosciences) to both aliquots and incubated them with 5% CO_2 at 37°C for 4 h. For testing intracellular IL-10 production, PBMCs were cultured for 24 h with complete medium containing 3 μg/ml CpG ODN (Invivogen). In the last 4 h of culture we added 50 ng/ml PMA, 750 ng/ml ionomycin, 0.7 μl of GolgiStop (BD Biosciences) and 2 μg/ml brefeldin A. After incubation, cells were washed with saline. PBMC were surface stained with anti-CD3-PerCP, anti-CD19-PeCy7, anti-CD45-APC (BD Biosciences) for 30 min at 4°C. For intracellular labeling, cells were washed in PBS and resuspended in 200 μl of cytofix/cytoperm (BD Biosciences). After 20 min at 4°C, cells were washed in Perm/Wash buffer (BD Biosciences), pellets resuspended and stained intracellularly with anti-TNFα-FITC (BD Biosciences), anti-IL-6-PE (BD Biosciences) or anti-IL-10-PE (Biolegend) for 30 min at 4°C and washed. Finally, cells were analyzed on a standard FACSCanto II instrument and analyzed in FACSDiva software (BD Biosciences). A minimum of 30 000 events were collected for analysis of antigen staining.

Supplementary Material

Supplementary Material is available at *HMG* online.

Acknowledgements

The authors thank the 'Red Española de Esclerosis Múltiple (REEM)' sponsored by the 'Fondo de Investigación Sanitaria' (FIS), Ministry of Science and Innovation, Spain, and the 'Ajuts per donar Suport als Grups de Recerca de Catalunya', sponsored by the 'Agència de Gestió d'Ajuts Universitaris i de Recerca' (AGAUR), Generalitat de Catalunya, Spain.

Conflict of Interest statement. None declared.

Funding

Q4

References

1. Lassmann, H. (2013) Pathology and disease mechanisms in different stages of multiple sclerosis. *J. Neurol. Sci.*, **333**, 1–4.
2. Dutta, R. and Trapp, B.D. (2007) Pathogenesis of axonal and neuronal damage in multiple sclerosis. *Neurology*, **68**, S22–S31.
3. Friese, M.A., Schattling, B. and Fugger, L. (2014) Mechanisms of neurodegeneration and axonal dysfunction in multiple sclerosis. *Nat. Rev. Neurol.*, **10**, 225–238.
4. Loleit, V., Biberacher, V. and Hemmer, B. (2014) Current and future therapies targeting the immune system in multiple sclerosis. *Curr. Pharm. Biotechnol.*, **15**, 276–296.
5. Comabella, M. and Martin, R. (2007) Genomics in multiple sclerosis—current state and future directions. *J. Neuroimmunol.*, **187**, 1–8.
6. Davis, R.S. (2007) Fc receptor-like molecules. *Annu. Rev. Immunol.*, **25**, 525–560.
7. Zhu, C., Sato, M., Yanagisawa, T., Fujimoto, M., Adachi, T. and Tsubata, T. (2008) Novel binding site for Src homology 2-containing protein-tyrosine phosphatase-1 in CD22 activated by B lymphocyte stimulation with antigen. *J. Biol. Chem.*, **283**, 1653–1659.
8. Jackson, T.A., Haga, C.L., Ehrhardt, G.R., Davis, R.S. and Cooper, M.D. (2010) FcR-like 2 Inhibition of B cell receptor-mediated activation of B cells. *J. Immunol.*, **185**, 7405–7412.
9. Haga, C.L., Ehrhardt, G.R., Boohaker, R.J., Davis, R.S. and Cooper, M.D. (2007) Fc receptor-like 5 inhibits B cell activation via SHP-1 tyrosine phosphatase recruitment. *Proc. Natl. Acad. Sci. U.S.A.*, **104**, 9770–9775.
10. Nitschke, L. (2005) The role of CD22 and other inhibitory co-receptors in B-cell activation. *Curr. Opin. Immunol.*, **17**, 290–297.
11. O'Connor, K.C., Appel, H., Bregoli, L., Call, M.E., Catz, I., Chan, J.A., Moore, N.H., Warren, K.G., Wong, S.J., Hafler, D.A. *et al.* (2005) Antibodies from inflamed central nervous system tissue recognize myelin oligodendrocyte glycoprotein, *J. Immunol.*, **175**, 1974–1982.
12. Weber, M. and Hemmer, B. (2010) Cooperation of B cells and T cells in the pathogenesis of multiple sclerosis. *Results Probl. Cell Differ.*, **51**, 115–126.
13. Fischer, M.T., Wimmer, I., Höftberger, R., Gerlach, S., Haider, L., Zrzavy, T., Hametner, S., Mahad, D., Binder, C.J., Krumbholz, M. *et al.* (2013) Disease-specific molecular events in cortical multiple sclerosis lesions. *Brain*, **136**, 1799–1815.
14. Magliozzi, R., Howell, O., Vora, A., Serafini, B., Nicholas, R., Puopolo, M., Reynolds, R. and Aloisi, F. (2007) Meningeal B-cell follicles in secondary progressive multiple sclerosis associate with early onset of disease and severe cortical pathology. *Brain*, **130**, 1089–1104.
15. Montalban, X., Sastre-Garriga, J., Tintoré, M., Brieva, L., Aymerich, F.X., Río, J., Porcel, J., Borràs, C., Nos, C. and Rovira, A. (2009) A single-center, randomized, double-blind, placebo-controlled study of interferon beta-1b on primary progressive and transitional multiple sclerosis. *Mult. Scler.*, **15**, 1195–1205.

16. De Stefano, N., Airas, L., Grigoriadis, N., Mattle, H.P., O'Riordan, J., Oreja-Guevara, C., Sellebjerg, F., Stankoff, B., Walczak, A., Wiendl, H. *et al.* (2014) Clinical relevance of brain volume measures in multiple sclerosis. *CNS Drugs*, **28**, 147–156.
17. Vidal-Jordana, A., Sastre-Garriga, J., Rovira, A. and Montalban, X. (2015) Treating relapsing-remitting multiple sclerosis: therapy effects on brain atrophy. *J. Neurol.*, in press.
18. Bielekova, B., Kadom, N., Fisher, E., Jeffries, N., Ohayon, J., Richert, N., Howard, T., Bash, C.N., Frank, J.A., Stone, L. *et al.* (2005) MRI as a marker for disease heterogeneity in multiple sclerosis. *Neurology*, **65**, 1071–1076.
19. Irizarry, R.A., Hobbs, B., Collin, F., Beazer-Barclay, Y.D., Antonellis, K.J., Scherf, U. and Speed, T.P. (2003) Exploration, normalization, and summaries of high density oligonucleotide array probe level data. *Biostatistics*, **4**, 249–264.
20. Ritchie, M.E., Phipson, B., Wu, D., Hu, Y., Law, C.W., Shi, W. and Smyth, G.K. (2015) limma powers differential expression analyses for RNA-sequencing and microarray studies. *Nucleic Acids Res.*, **43**, e47.
21. Livak, K.J. and Schmittgen, T.D. (2001) Analysis of relative gene expression data using real-time quantitative PCR and the 2(-Delta Delta C(T)) Method. *Methods*, **25**, 402–408.